Investigation of the Inhibition Effect of Nontoxic Purine Derivatives on the Carbon Steel Corrosion in 0.5 M H$_2$SO$_4$ Solution

Ahmed A. Farag

Petroleum Applications Department, Egyptian Petroleum Research Institute (EPRI)
1 Ahmed El-Zomor St., Nasr City, 11727, Cairo, Egypt

Abstract: *The behavior of carbon steel in 0.5 M H$_2$SO$_4$ in the presence of novel purine inhibitors namely 1H-pyrazolo[3,4-d]pyrimidin-4(2H)-one (P1) and 6-[(1-methyl-4-nitro-5-imidazolyl)sulfanyl]purine (P2) in the concentration range (1×10^{-4} − 5×10^{-3} M) was studied using weight loss, open circuit potential, potentiodynamic polarization electrochemical impedance spectroscopy (EIS) techniques. Potentiodynamic polarization shows that P1 and P2 act as mixed-type inhibitors. The adsorption of inhibitors on metal followed Langmuir's adsorption isotherm. SEM images showed that the inhibitor molecules form a good protective film on the carbon steel surface.*

Keywords: Carbon steel, Acid corrosion, Polarization, EIS.

1. Introduction

Acid solutions are widely used in the industry, some of the important fields of application being acid pickling of iron and steel, chemical cleaning and processing, ore production and oil well acidification [1]. Because of the general aggression of acid solutions, inhibitors are commonly used to reduce the corrosive attack on metallic materials. Most well-known acid inhibitors are organic compounds containing nitrogen, sulfur, and oxygen atoms. Among them, nitrogen containing heterocyclic compounds is considered to be effective corrosion inhibitors for steel in acid media [2]. N-heterocyclic compound inhibitors act by adsorption on the metal surface, and the adsorption of N-heterocyclic inhibitor takes place through nitrogen heteroatom, as well as those with triple or conjugated double bonds or aromatic rings in their molecular structures. Although N-heterocyclic organic compounds have good anti-corrosive activity; they are highly toxic to both human beings and environment [3].

The safety and environmental issues of corrosion inhibitors arisen in industries has always been a global concern. These toxic effects have led to the use of eco-friendly and harmless N-heterocyclic compounds as inhibitors. As an important N-heterocyclic compound, purine and purine derivatives are non-toxic and biodegradable; this makes the investigation of their inhibiting properties significant within the context of the current priority to produce eco-friendly inhibitors. However, data on the use of purine and purine derivatives as corrosion inhibitors are not so plentiful. In addition, higher attentions have been revealed in the study of the inhibiting effects on the steel of purine and purine derivative in HCl medium, lower attentions in H$_2$SO$_4$ medium, especially in a wide concentration range of H$_2$SO$_4$ solution.

The aim of this work is to investigate a novel purine inhibitors namely, 1H-pyrazolo[3,4-d]pyrimidin-4(2H)-one (P1) and 6-[(1-methyl-4-nitro-5-imidazolyl)sulfanyl]purine (P2) as the corrosion inhibitor for carbon steel in 0.5 M H$_2$SO$_4$ using different techniques.

2. Experimental

The inhibitors solutions were prepared in 0.5 M H$_2$SO$_4$. The corrosion tests were performed in 0.5 M H$_2$SO$_4$ in the absence and presence of various concentrations of inhibitors. The aggressive solution of 0.5 M H$_2$SO$_4$ was prepared by dilution of analytical grade, 98% H$_2$SO$_4$ with distilled water. For each experiment, a freshly prepared solution was used under air atmosphere without stirring at 298 K.

The tests were performed on carbon steel of the following composition (wt.%): 0.07% C, 0.24% Si, 1.35% Mn, 0.017% P, 0.005% S, 0.16% Cr, 0.18% Ni, 0.12% Mo, 0.01% Cu and the remainder Fe.

The carbon steel coupons of 7.0 cm × 2.0 cm × 0.03 cm were abraded with a series of emery paper beginning from 400 to 1200, degreased with acetone, rinsed with distilled water and dried in hot air. After weighing accuracy, the specimens were immersed in 150 ml beaker, which contained 150 ml sulfuric acid with and without the addition of various concentrations of inhibitors. All the aggressive acid solutions were open to air. After 24 h, the specimens were taken out, washed, dried, and weighed accurately. In order to get good reproducibility, the experiments were carried out in triplicate, and the average weight loss of three parallel carbon steel coupons was reported. Then the tests were repeated at different temperatures. The corrosion rate (ν) was calculated from the following equation:

$$\nu = \frac{W}{St} \qquad (1)$$

where W is the average weight loss of three parallel carbon steel coupons, S the total area of one steel coupon, and t is immersion time (24 h). With the calculated corrosion rate, the inhibition efficiency (η_g) of inhibitors on the corrosion of carbon steel was calculated as follows [4]:

$$\eta_g = \frac{\nu_0 - \nu}{\nu_0} \times 100 \qquad (2)$$

where ν_0 and ν are the values of the corrosion rate without

and with addition of the inhibitor, respectively.

The electrochemical measurements were carried out using Volta lab 40 (Tacussel-Radiometer PGZ301) potentiostate and controlled by Tacussel corrosion analysis software model (Voltamaster 4) at under static condition. The corrosion cell used had three electrodes. The reference electrode was a saturated calomel electrode (SCE). A platinum electrode was used as auxiliary electrode. Carbon steel coupons having the area of 1 cm^2 were used as a working electrode. The working electrode was immersed in test solutions for 30 minutes to a establish steady state open circuit potential (E_{ocp}). After measuring the E_{ocp}, the electrochemical measurements were performed. The EIS experiments were conducted in the frequency range with high limit of 10^5 Hz and different low limit 10^{-2} Hz at open circuit potential. The polarization curves were obtained in the potential range from −900 to −200 mV(SCE) with 0.5 mV s^{-1} scan rate.

3. Results and Discussion

3.1. Gravimetric Measurements

3.1.1. Effect of Inhibitor Concentration
Table 1 showed the values of corrosion rates v (mg cm^{-2} h^{-1}), surface coverage (θ) and inhibition efficiencies (η_g) obtained from gravimetric measurements in the absence and presence of various concentrations of inhibitors at 298 K for 24 h immersion in 0.5 M H$_2$SO$_4$. It is clear that the weight loss decreased (i.e. ν is decreased) and η_g increased with increasing concentration of inhibitors. The maximum η_g values of 5×10^{-3} M of P1 and P2 were found 90.6% and 95.3%, respectively. The inhibition of corrosion occurs due to the larger surface coverage (θ) of the metal surface by inhibitor molecules [5].

Table 1: Corrosion parameters obtained from gravimetric measurements

Conc.(M)	P1			P2		
	v (mg cm^{-2} h^{-1})	θ	η_g (%)	v (mg cm^{-2} h^{-1})	θ	η_g (%)
Blank	1.381	—	—	1.381	—	—
1×10^{-4}	0.655	0.526	52.6	0.493	0.643	64.3
5×10^{-4}	0.331	0.76	76	0.176	0.872	87.2
1×10^{-3}	0.198	0.857	85.7	0.076	0.945	94.5
5×10^{-3}	0.13	0.906	90.6	0.065	0.953	95.3

3.1.2. Effect of Temperature
Gravimetric measurements were taken at various temperatures (298–328 K) in the absence and presence of optimum concentration (5×10^{-3} M) of P1 and P2 for 24 h of immersion in 0.5 M H$_2$SO$_4$. The results obtained are listed in Table 2.

Table 2: Corrosion Parameters obtained from gravimetric measurements of P1 and P2 at different temperatures

Temperature	Parameters	Blank	P1	P2
298 K	v (mg cm^{-2} h^{-1})	1.381	0.13	0.065
	θ	—	0.906	0.953
	η_g (%)	—	90.6	95.3
308 K	v (mg cm^{-2} h^{-1})	1.879	0.314	0.191
	θ	—	0.833	0.899
	η_g (%)	—	83.3	89.9
318 K	v (mg cm^{-2} h^{-1})	2.932	0.61	0.465
	θ	—	0.792	0.841
	η_g (%)	—	79.2	84.1
328 K	v (mg cm^{-2} h^{-1})	4.964	1.138	1.012
	θ	—	0.771	0.796
	η_g (%)	—	77.1	79.6

Inspection the data of Table 2 revealed that the corrosion rate (v) increases with increase in temperature. Dissolution of carbon steel is generally accompanied by evolution of hydrogen gas in acidic media and corrosion rate is accelerated by the increase in temperature, resulting in higher dissolution of the carbon steel. It is clear from the Table 2 that η_g decreases with increasing the solution temperature from 298 to 328 K. The decrease in η_g might be due desorption of the inhibitor molecules from the carbon steel surface.

3.1.3. Adsorption Isotherms
The values of surface coverage and inhibitor concentration were used to obtain the isotherms [6]. Various isotherms have been tested, but the best fit was obtained for Langmuir isotherm. The Langmuir isotherm is given by:

$$\frac{C}{\theta} = \frac{1}{K_{ads}} + C \qquad (3)$$

where C is the inhibitor concentration, θ is the surface coverage ($\theta = \eta_g / 100$), K_{ads} is the equilibrium constant of adsorption process. Plots of C/θ against C yield straight lines as shown in Figure 1, and the corresponding linear regression parameters are listed in Table 3. Both linear correlation coefficient (r) and slope are close to 1, indicating the adsorption of two inhibitors on the carbon steel surface obeys Langmuir adsorption isotherm. The adsorptive equilibrium constant (K_{ads}) can be calculated from the reciprocal of the intercept of C/θ–C curve.
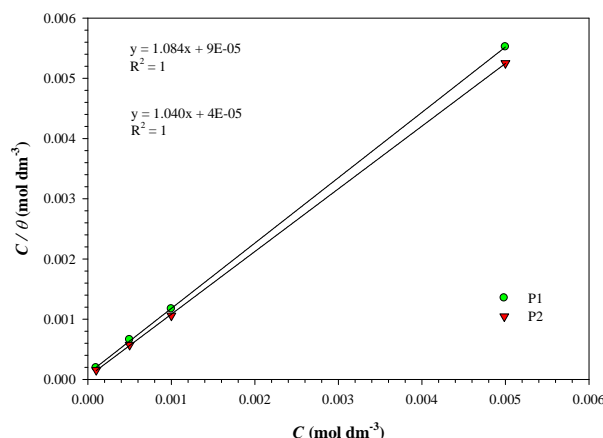

Figure 1: Langmuir adsorption plots of carbon steel in 0.5 M H$_2$SO$_4$ containing the investigated inhibitors at 298 K

Generally, a large value of K_{ads} attribute to the stronger and more stable adsorbed layer formed on the metal surface. The standard free energy of adsorption (ΔG_{ads}^{o}) can be given as the following equation:

$$\Delta G_{ads}^{o} = -RT \ln(55.5 K_{ads}) \qquad (4)$$

where, R is the gas constant (8.314 J mol^{-1} K^{-1}), T the absolute temperature (K), and the value 55.5 is the concentration of water in solution expressed in molar. The high values of cards and negative values of ΔG_{ads}^{o} suggested that, inhibitor molecules strongly adsorb on the carbon steel surface.

Table 3: Adsorption equilibrium constant and standard free energy of adsorption at 298 K

Inhibitor	Linear correlation coefficient (r)	Slope	K_{ads} (M^{-1})	$-\Delta G_{ads}^{o}$ (kJ mol^{-1})
P1	1	1.084	11×10^{6}	51
P2	1	1.040	25×10^{6}	53

Values of ΔG_{ads}^{o} around -20 kJ mol^{-1} or lower are consistent with the electrostatic interaction between charges inhibitor molecules and the charged metal surface (physisorption); those around -40 kJ mol^{-1} or higher involve charge sharing or transfer from the inhibitor molecules to the metal surface to form a coordinate type of bond (chemisorption) [7]. The obtained ΔG_{ads}^{o} values were -51 and -53 kJ mol^{-1} for P1 and P2, respectively. This indicates that the adsorption takes place mainly through the donor–acceptor bond between unpaired electrons of inhibitor molecules and the carbon steel surface (chemisorption).

3.1.4. Thermodynamic Activation Parameters
Arrhenius and transition state equations were used to know the dependence of corrosion rate on temperature:

$$v = A \exp\left(\frac{-E_a}{RT}\right) \qquad (5)$$

$$v = \frac{RT}{Nh} \exp\left(\frac{\Delta S^*}{R}\right) \exp\left(\frac{-\Delta H^*}{RT}\right) \qquad (6)$$

where A is the pre-exponential factor, E_a represents apparent activation energy, N is the Avogadro's number, h is the Plank's constant, ΔS^* is the entropy of activation and ΔH^* is the enthalpy of activation.

y = -1811x + 6.188
R² = 0.979

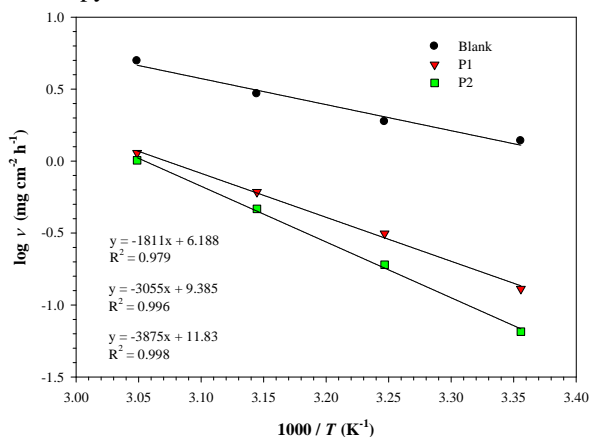y = -3055x + 9.385
R² = 0.996

y = -3875x + 11.83
R² = 0.998

Figure 2: Arrhenius plot for carbon steel dissolution in absence and presence investigated inhibitors

A plot of log$v$ versus $1/T$ gave a straight line as shown in Figure 2 with a slope of (E_a/2.303R) and their activation energy values are listed in Table 4. The data given in the Table 4 shows that E_a for the corrosion of carbon steel in H$_2$SO$_4$ solution is higher in inhibiting solution than those in the free acid solution, which is due to the adsorption of investigated inhibitors on the carbon steel surface. Also the higher values of E_a in inhibited solution might be correlated with the increased thickness of the double layer, which enhances the activation energy of the corrosion process [8].
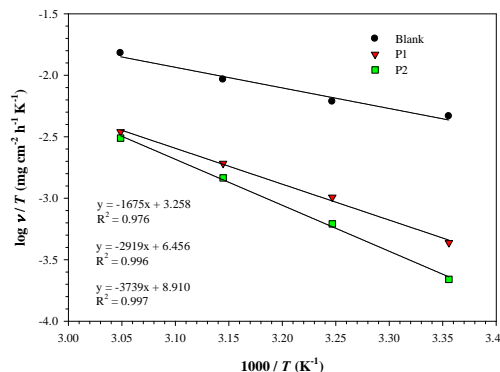

y = -1675x + 3.258
R² = 0.976

y = -2919x + 6.456
R² = 0.996

y = -3739x + 8.910
R² = 0.997

Figure 3: Transition state plot for carbon steel dissolution in absence and presence investigated inhibitors.

Table 4: Activation parameters in the absence and presence of optimum concentrations (5×10^{-3} M) of P1 and P2

Inhibitor	E_a (kJ mol^{-1})	ΔH^* (kJ mol^{-1})	$-\Delta S^*$ (J K^{-1} mol^{-1})
Blank	34.7	32.1	135.2
P1	58.5	55.9	73.9
P2	74.2	71.6	27.0

A plot of log v/T against $1/T$ gives straight lines with a slope value of (ΔH^*/2.303R) and an intercept of [log(R/Nh)) + (ΔH^*/2.303R)] as in Figure 3, from which the values of ΔH^* and ΔS^* were calculated and given in Table 4. Inspection of these data reveals that the ΔH^* values for the dissolution reaction of carbon steel in 0.5 M H$_2$SO$_4$ in the presence of inhibitors are higher than that in the absence of inhibitors. The positive signs of ΔH^* reflect that the dissolution of carbon steel is slow in the presence of inhibitor [9]. The values of E_a and ΔH^* enhance in the presence of inhibitor suggesting that the energy barrier of corrosion reaction increases. This means that the corrosion reaction will further be pushed to surface sites that are characterized by progressively higher values of E_a as the concentration of the inhibitor becomes greater [10]. The values of ΔS^* increase in presence of inhibitor as compared with uninhibited solution (Table 4). This was due to increases in randomness on going from reactants to the activated complex. This might be the results of the adsorption of organic inhibitor molecules from the H$_2$SO$_4$ solution and could be regarded as a quasi-substitution process between the organic compound in the aqueous phase and water molecules at the electrode surface [11]. In this situation, the adsorption of organic inhibitor was accompanied by desorption of water molecules from the surface. Thus the increase in entropy of activation was attributed to the increase in solvent entropy [12].

3.2. Electrochemical Measurements

3.2.1. Potentiodynamic Polarization Measurements

The effect of increased concentration of P1 and P2 on the polarization curves of carbon steel in 0.5 M H_2SO_4, at 298 K is represented in Figures 4 & 5, respectively. The electrochemical parameters such as corrosion potential (E_{corr}), corrosion current density (i_{corr}), cathodic Tafel constant (β_c), anodic Tafel slope (β_a) and inhibition efficiency (η_p) are calculated and given in Table 5. The η_p was calculated from polarization measurements according to the following relation [13]:

$$\eta_p = \left(\frac{i_{corr} - i_{corr}^o}{i_{corr}} \right) \times 100 \qquad (7)$$

where i_{corr} and i_{corr}^o are uninhibited and inhibited corrosion current densities, respectively.
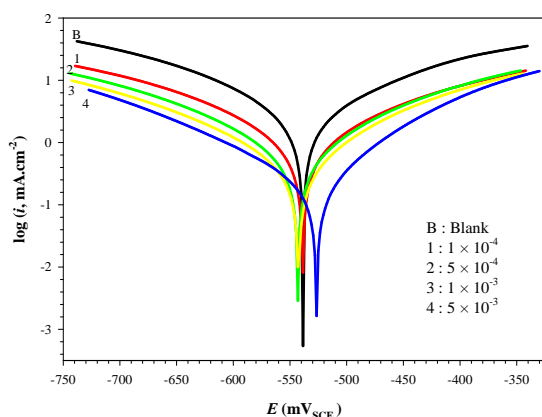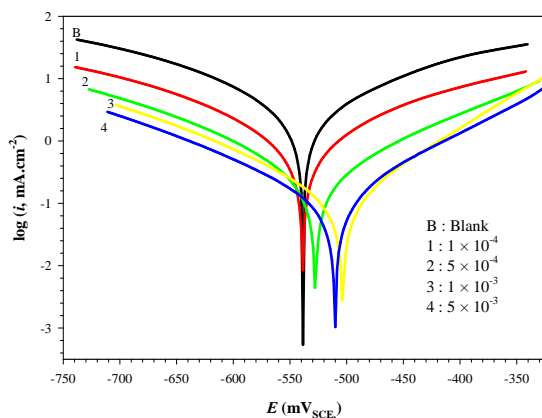
Table 5: Potentiodynamic polarization parameters of P1 and P2 at 298 K

Inhibitor	C (M)	$-E_{corr}$ (mV$_{SCE}$)	i_{corr} (mA cm^{-2})	β_a (mV dec^{-1})	$-\beta_c$ (mV dec^{-1})	η_p (%)
Blank	0	538.5	6.1184	248.5	232.9	—
P1	1×10^{-4}	538.7	2.9023	258.2	231.5	52.6
	5×10^{-4}	543.1	1.4259	210.4	229.5	76.7
	1×10^{-3}	542.5	0.8777	156.6	186.5	85.7
	5×10^{-3}	526.5	0.5859	109.9	158.1	90.4
P2	1×10^{-4}	538.7	2.1987	223	208.2	64.1
	5×10^{-4}	527.7	0.7655	166.1	178.6	87.5
	1×10^{-3}	503.6	0.3583	102.7	155.4	94.1
	5×10^{-3}	510.5	0.3022	118.7	162.7	95.1

It is clear that the i_{corr} decrease with the increasing of the inhibitor concentration; this indicates that purine compounds are adsorbed on the metal surface and hence inhibition occurs. The polarization curves (Figures 4 & 5) show that P1 and P2 has an effect on both, the cathodic and anodic slopes (β_c and β_a) and suppressed both cathodic and anodic processes. This indicates a modification of the mechanism of cathodic hydrogen evolution as well as anodic dissolution of iron, which suggest that inhibitor powerfully inhibits the corrosion process of carbon steel, and its ability as corrosion inhibitor is enhanced as its concentration is increased. The suppression of cathodic process can be due to the covering of the surface with monolayer due to the adsorbed inhibitor molecules. It can also be seen from Table 5 that the anodic Tafel slope (β_a) decreases in the presence of inhibitors. This observation may be ascribed to changes in the charge transfer coefficient for the anodic dissolution of iron by virtue of the presence of an additional energy barrier due to the presence of adsorbed inhibitor. Further inspection of Table 5 also reveals that E_{corr} values do not show any significant change in the presence of various concentrations of the inhibitor suggesting that P1 and P2 are mixed-type in 0.5 M H_2SO_4, which influences both metal dissolution and hydrogen evolution [14].

Figure 4: Polarization curves in the absence and presence of various concentrations of P1

Figure 5: Polarization curves in the absence and presence of various concentrations of P2

3.2.2. Electrochemical Impedance Spectroscopy (EIS)

Figures 6 & 7 show the Nyquist plots for carbon steel in 0.5 M H_2SO_4 in the absence and presence of P1 and P2 at 298 K, respectively.
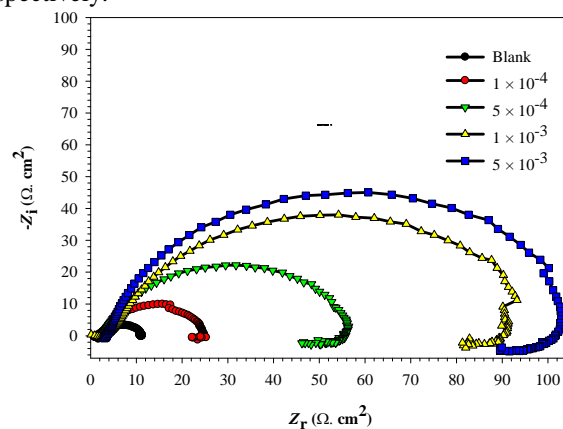

Figure 6: Nyquist plots in the absence and presence of various concentrations of P1
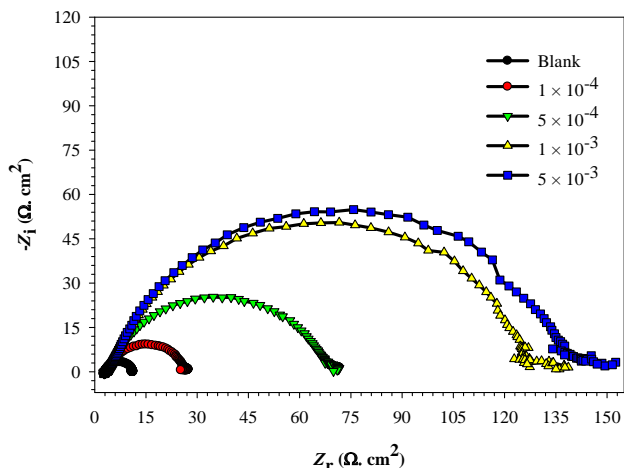
Figure 7: Nyquist plots in the absence and presence of various concentrations of P2

The impedance diagrams consist of a large capacitive loop at high frequencies followed by a small inductive loop at low frequency values. The high frequency capacitive loop is usually related to the charge transfer of the corrosion process and double layer behavior. On the other hand, the low frequency inductive loop may be attributed to the relaxation process obtained from adsorption species like $FeSO_4$ or inhibitor species on the electrode surface. It might be also attributed to the re-dissolution of the passivated surface at low frequencies. Furthermore, the diameter of the capacitive loop in the presence of inhibitors is bigger than that with the uninhibited solution and increases with the inhibitor concentrations. This indicates that the impedance of carbon steel corrosion increases with the inhibitor concentration. The capacitive loops are not perfect semicircles which attributed to the frequency dispersion effect as a result of the roughness and inhomogeneous of electrode surface. The electrochemical parameters derived from Nyquist plots are calculated and listed in Table 6. The values of charge transfer resistance (R_t) were given by subtracting the high frequency impedance from the low frequency one as follow [15]:

$$R_t = Z_{re}(at\ low\ frequency) - Z_{re}(at\ high\ frequency) \quad (8)$$

The values of electrochemical double layer capacitance (C_{dl}) were calculated at the frequency, f_{max}, at which the imaginary component of the impedance is maximal ($-Z_{max}$) by the following equation:

$$C_{dl} = (2\pi f_{max} R_t)^{-1} \quad (9)$$

The values of percentage inhibition efficiency (η_i) were calculated from the values of R_t according to the following equation [16]:

$$\eta_i = \left(\frac{R_t - R_t^o}{R_t} \right) \times 100 \quad (10)$$

where R_t and R_t^o are the values of the charge transfer resistance in the presence and absence of inhibitor, respectively.

Table 6: Electrochemical impedance parameters of P1 and P2 at 298 K

Inhibitor	C (M)	R_s (ohm.cm²)	R_t (ohm.cm²)	C_{dl} (μF cm⁻²)	η_i (%)
Blank	0	2.9	9.8	348.5	—
P1	1×10^{-4}	2	22.45	152.3	56.4
	5×10^{-4}	3.2	50.55	70.4	80.6
	1×10^{-3}	3.6	82.45	49.5	88.1
	5×10^{-3}	3.6	91.14	38.4	89.3
P2	1×10^{-4}	3.8	23.3	148.7	57.9
	5×10^{-4}	3.6	66.4	61.8	85.2
	1×10^{-3}	3.3	124.8	36.6	92.2
	5×10^{-3}	3.7	139.9	29.1	93

The impedance data listed in Table 6 indicate that the values of both R_t and η_i are found to increase by increasing the inhibitor concentration, while the values of C_{dl} are found to decrease. This behavior was the result of an increase in the surface coverage by the inhibitor molecules, which led to an increase in the inhibition efficiency. The decrease in C_{dl} values may be considered in terms of Helmholtz model [17]:

$$C_{dl} = \frac{\varepsilon \varepsilon_0}{d} \times S \quad (11)$$

where ε_o is the permittivity of space (8.854×10^{-12} Fm⁻¹), ε is the local dielectric constant, d is the thickness of the film and S is the surface area of the electrode. In fact, the decrease in C_{dl} values can result from a decrease in local dielectric constant and/or an increase in the thickness of the electrical double layer. The impedance spectra for the Nyquist plots were analyzed by fitting to the equivalent circuit model shown in Figure 8, which has been used previously to model the steel/acid interface [18].
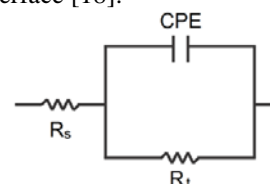

**Figure 8:** Equivalent circuit model used to fit the impedance data for carbon steel

The circuit comprises a solution resistance R_s shorted by a constant phase element (CPE) that is placed in parallel to the charge transfer resistance R_t. The value of the charge transfer resistance is indicative of electron transfer across the interface. The use of the CPE, has been extensively described in the literature [19,20] and is employed in the model to compensate for the inhomogeneities in the electrode surface as depicted by the depressed nature of the Nyquist semicircle. The introduction of such a CPE is often used to interpret data for rough solid electrodes. The impedance, Z, of the CPE is:

$$Z_{CPE} = \left[Q(j\omega)^n \right]^{-1} \quad (12)$$

where the coefficient Q is a combination of properties related to different physical phenomena like surface inhomogeneousness, electro-active species, inhibitor adsorption, porous layer formation, etc., j is an imaginary number ($j^2 = -1$), ω is the angular frequency ($\omega = 2\pi f$) and the exponent n has values between -1 and 1. A value of -1 is a characteristic for an inductance, a value 1 corresponds to a resistor, and a value of 0.5 can be assigned to diffusion phenomenon [21].

3.4. Explanation for Inhibition

The gravimetric and electrochemical results show that, P1 and P2 are efficient for carbon steel corrosion in 0.5 M H_2SO_4. The better performance was seen in the case of P2 ($C_9H_7N_7O_2S$) than P1 ($C_5H_4N_4O$). The higher inhibition efficiency of P2 can be explained by the presence of the extra imidazole group and sulfur atom in its molecular structure, which is considered to be active centers of adsorption. The presence of such groups in molecular structure of inhibitor molecule increases electron density on adsorption centers and leading to an easier electron transfer from the functional group to the metal surface, producing greater coordinate bonding and higher inhibition efficiency. The inhibition effect of investigated purine inhibitors in H_2SO_4 solution can be explained as follows: purine inhibitor might be protonated in the acid solution as following:

$$Inh + xH^+ \leftrightarrow \left[InhH_x\right]^{x+} \qquad (13)$$
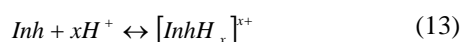
Thus, in aqueous acidic solutions, the inhibitor exists either as: (1) neutral molecules or (2) in the form of cations (protonated inhibitor). Generally, two modes of adsorption could be considered. The neutral inhibitor may be adsorbed on the metal surface via the adsorption mechanism, involving the displacement of water molecules from the metal surface and the sharing electrons between the heteroatom's and iron surface. The inhibitor molecules can be also adsorbed on the metal surface on the basis of donor–acceptor interactions between π-electrons of the heterocyclic and vacant d-orbitals of iron surface. In another hand, could adsorb on the metal surface, and then the protonated inhibitor may adsorb through electrostatic interactions between the positively charged inhibitor and already adsorbed sulfate ions [22]. It should be noted that the molecular structure of poronated inhibitor remains unchanged with respect to its neutral form, the heteroatoms on the ring remaining strongly blocked, so when protonated purine inhibitor adsorbed on the metal surface, co-ordinate bond may be formed by partial transference of electrons from the polar heteroatom's to the metal surface.

4. Conclusions

P1 and P2 act as a good inhibitor for the corrosion of carbon steel in 0.5 M H_2SO_4, and the inhibition efficiency increase with the inhibitor concentration, while decrease with the temperature. The adsorption of the P1 and P2 on the carbon steel surface obeys the Langmuir adsorption isotherm. The potentiodynamic polarization curves indicated that P1 and P2 behave as a mixed-type inhibitor. EIS results indicate that the C_{dl} decrease when these inhibitors are added; this due to adsorption of these inhibitors on the steel surface.

5. Acknowledgement

References

[1] Shuduan Deng, Xianghong Li, "Inhibition by Ginkgo leaves extract of the corrosion of steel in HCl and H_2SO_4 solutions," Corros. Sci. 55 (2012) 407–415.

[2] H.A. Mohamed, A.A. Farag, B.M. Badran, "Friendly to Environment Heterocyclic Adducts as Corrosion Inhibitors for Steel in Water-Borne Paints," J. Appl. Polym. Sci. 117 (2010) 1270-1278.

[3] Xianghong Li, Shuduan Deng, Hui Fu, Guannan Mu, "Inhibition effect of 6-benzylaminopurine on the corrosion of cold rolled steel in H_2SO_4 solution," Corros. Sci. 51 (2009) 620–634.

[4] M.A. Migahed, A.A. Farag, S.M. Elsaed, R. Kamal, M. Mostfa, H. Abd El-Bary, "Synthesis of a new family of Schiff base nonionic surfactants and evaluation of their corrosion inhibition effect on X-65 type tubing steel in deep oil wells formation water," Mater. Chem. Phys. 125 (2011) 125–135.

[5] T.P. Zhao, G.N. Mu, "The adsorption and corrosion inhibition of anion surfactants on aluminium surface in hydrochloric acid," Corros. Sci. 41 (1999) 1937–1944.

[6] O. O. Xomet, N. V. Likhanova, M. A. D. Anguilar, E. Arce, H. Dorantes, P. A. Lozada, "Synthesis and corrosion inhibition of α-amino acids alkylamides for mild steel in acidic environment," Mater. Chem. Phys., 110 (2008) 344-351.

[7] R. Solmaz, G. Kardas, B. Yazıcı, M. Erbil, "Adsorption and corrosion inhibitive properties of 2-amino-5-mercapto-1,3,4-thiadiazole on mild steel in hydrochloric acid media," Colloids and Surfaces A: Physicochem. Eng. Aspects, 312 (2008) 7–17.

[8] S. Martinez, I. Stern, "Thermodynamic characterization of metal dissolution and inhibitor adsorption processes in the low carbon steel/mimosa tannin/sulfuric acid system," Appl. Surf. Sci. 199 (2002) 83–89.

[9] N. M. Guan, L. Xueming, L. Fei, "Synergistic inhibition between o-phenanthroline and chloride ion on cold rolled steel corrosion in phosphoric acid," Mater. Chem. Phys., 86 (2004) 59-68.

[10] S. S. Abd El Rehim, M. A. M. Ibrahim, K. F. Khalid, "The inhibition of 4-(2′-amino-5′-methylphenylazo) antipyrine on corrosion of mild steel in HCl solution," Mater. Chem. Phys., 70 (2001) 268-273.

[11] M. Sahin, S. Bilgic, H. Yilmaz, "The inhibition effects of some cyclic nitrogen compounds on the corrosion of the steel in NaCl mediums," Appl. Surf. Sci., 195 (2002) 1-7.

[12] B. Ateya, B. E. El-Anadouli, F. M. El-Nizamy, "The adsorption of thiourea on mild steel," Corros. Sci., 24 (1984) 509-515.

[13] Ahmed A. Farag, M.R. Noor El-Din, "The adsorption and corrosion inhibition of some nonionic surfactants on API X65 steel surface in hydrochloric acid," Corros. Sci. 64 (2012) 174–183.

[14] M.A. Quraishi, D. Jamal, "Dianils as new and effective corrosion inhibitors for mild steel in acidic solutions," Mater. Chem. Phys. 78 (2003) 608-613.

[15] Ahmed M. Al-Sabagh, Notaila M. Nasser, Ahmed A. Farag, Mohamed A. Migahed, Abdelmonem M.F. Eissa, Tahany Mahmoud, "Structure effect of some amine derivatives on corrosion inhibition efficiency for carbon

steel in acidic media using electrochemical and Quantum Theory Methods," Egyptian Journal of Petroleum 22 (2013) 101–116.

[16] M.A. Migahed, A.A. Farag, S.M. Elsaed, R. Kamal, H.A. El-Bary, "Corrosion inhibition of steel pipelines in oil well formation water by a new family of nonionic surfactants," Chem. Eng. Commun. 199 (2012) 1335-1356.

[17] Ahmed A. Farag, M.A. Hegazy, "Synergistic inhibition effect of potassium iodide and novel Schiff bases on X65 steel corrosion in 0.5 M H_2SO_4," Corros. Sci. 74 (2013) 168–177.

[18] M. Kissi, M. Bouklah, B. Hammouti, M. Benkaddour, "Establishment of equivalent circuits from electrochemical impedance spectroscopy study of corrosion inhibition of steel by pyrazine in sulphuric acidic solution," Appl. Surf. Sci. 252 (2006) 4190-4197.

[19] L. Larabi, Y. Harek, O. Benali, S. Ghalem, "Hydrazide derivatives as corrosion inhibitors for mild steel in 1 M HCl," Prog. Org. Coat. 54 (2005) 256-262.

[20] Popova, E. Sokolova, S. Raicheva, M. Christov, "AC and DC study of the temperature effect on mild steel corrosion in acid media in the presence of benzimidazole derivatives," Corros. Sci. 45 (2003) 33-58.

[21] Hulya Keles, Mustafa Keles, Ilyas Dehri, Osman Serindag, "The inhibitive effect of 6-amino-m-cresol and its Schiff base on the corrosion of mild steel in 0.5 M HCI medium," Mater. Chem. Phys. 112 (2008) 173–179.

[22] F. Bentiss, M. Traisnel, M. Lagrenée, "The substituted 1,3,4-oxadiazoles: a new class of corrosion inhibitors of mild steel in acidic media," Corros. Sci. 42 (2000) 127–146.

Author Profile

Ahmed A. Farag received the B.Sc., Master and Ph.D. degrees in Chemistry from Science Faculty, Al-Azhar University/ Egypt in 2002, 2007 and 2011, respectively. I worked in National Research Center (NRC), Polymers and Pigments Department/Egypt until 2007. Now I am working in Egyptian Petroleum Research Institute (EPRI), Petroleum Applications Department/Egypt from 2007 until now.